

Factors Controlling Mud Floc Settling Velocity in a Highly Turbid Macrotidal Fluvial-Estuarine System



Key Points:

- In such hyper-turbid system, the suspended sediment concentration predominantly drives the settling dynamics of suspended sediment
- The turbulent shear appeared to be a control parameter of secondary importance
- A common prediction law can be found for the whole system

Correspondence to:

S. Defontaine,
sophie.defontaine@cerema.fr

Citation:

Defontaine, S., Jalón-Rojas, I., Sottolichio, A., Gratiot, N., Legout, C., & Lienart, C. (2024). Factors controlling mud floc settling velocity in a highly turbid macrotidal fluvial-estuarine system. *Journal of Geophysical Research: Oceans*, 129, e2024JC021558. <https://doi.org/10.1029/2024JC021558>

Received 8 JUL 2024
 Accepted 20 SEP 2024

Author Contributions:

Conceptualization: Sophie Defontaine

Investigation: Sophie Defontaine

Methodology: Sophie Defontaine, Isabel Jalón-Rojas, Aldo Sottolichio, Nicolas Gratiot, Cédric Legout, Camilla Lienart

Validation: Isabel Jalón-Rojas, Aldo Sottolichio, Nicolas Gratiot, Cédric Legout

Writing – original draft: Sophie Defontaine

Writing – review & editing: Isabel Jalón-Rojas, Aldo Sottolichio, Nicolas Gratiot, Cédric Legout, Camilla Lienart

Sophie Defontaine^{1,2,3} , Isabel Jalón-Rojas¹ , Aldo Sottolichio¹ , Nicolas Gratiot⁴, Cédric Legout⁴ , and Camilla Lienart¹

¹University Bordeaux, CNRS, Bordeaux INP, EPOC, UMR 5805, Pessac, France, ²Now at Cerema, RHITME Research Team, Margny Les Compiègne, France, ³Now at University Rouen Normandie, Université Caen Normandie, CNRS, Normandie University, M2C UMR 6143, Rouen, France, ⁴University Grenoble Alpes, CNRS, IRD, Grenoble INP, IGE, Grenoble, France

Abstract This study assesses the settling dynamics of suspended sediments along the hyper-turbid Gironde Garonne fluvial-estuarine system, with an innovative optical SCAF instrument (System of Characterization of Aggregates and Floccs). Two fields campaigns were carried out to determine the settling velocity and properties of suspended sediments during a semi-diurnal tidal cycle, as well as hydrodynamic conditions and water properties. The two sampling stations were representative of two regions: a tidal river dominated by fresh water and an estuary affected by salty or brackish waters. A high spatial variability of the settling velocity was observed along the fluvial-estuarine system and vertically along the water column. Settling velocities ranged from 0.02 to 0.4 mm/s. This study confirms that in hyper-turbid systems, the suspended sediment concentration (SSC) is predominantly driving the settling dynamics of suspended sediment. Threshold concentrations have been defined for the flocculation and hindered regimes where the settling velocity may vary by one order of magnitude. Although in natural environments it is difficult to distinguish between the effects of SSC and turbulence (as they are correlated), in the Gironde-Garonne system the turbulent shear G seems to affect the settling of suspended sediment to a lower extent. Settling velocity variations cannot be directly correlated to salinity or organic matter content. Despite differences in hydrodynamic and environmental conditions in fluvial and estuarine regions, a common prediction law has been found to estimate settling velocity of suspended sediment as a function of suspended sediment concentration.

Plain Language Summary Estuaries and rivers are biotically rich environments strongly impacted by human activities. Mud trapping capacity of such systems has a major influence on water quality by reducing light availability, promoting oxygen depletion and by trapping adsorbed contaminants, bacteria and nutrients. A key dynamical parameter impacting the trapping of mud is the sediment settling velocity. Sediment settling is influenced by a wide range of environmental factors such as salinity, sediment concentration, turbulence of the flow and organic matter. This manuscript presents sediment settling data from field surveys carried out along the Garonne River—Gironde Estuary system (France), where large quantities of mud are trapped during the dry season. It highlights the driving role of sediment concentration on the settling dynamics along the entire system, despite the hydrodynamics and water properties of riverine waters differing from the estuarine waters. The turbulence of the flow appeared to be of secondary importance. An unique empirical prediction law has been established for the whole system contrary to other systems around the world. An improved understanding of sediment fluxes contributes to effective waterways management and the preservation of essential ecological environments.

1. Introduction

The transport of particles in estuaries and tidal rivers is governed by tidal currents, estuarine circulation, river discharge and particle characteristics. The fine sediment trapping capacity of such systems leads to the formation of estuarine turbidity maxima (ETM), which are main features and have a major influence on water quality by reducing light availability, promoting oxygen depletion and trapping adsorbed contaminants, bacteria and nutrients (Fox et al., 2014; Geyer & Ralston, 2018; Hassard et al., 2016). A better understanding and prediction ability of cohesive sediment fluxes is thus crucial for waterway management and ecological purposes.

A unique attribute of cohesive sediment is its potential to form flocs of different sizes and densities, representing an important dynamic process that greatly impacts cohesive sediment fluxes in riverine and estuarine

© 2024. The Author(s).

This is an open access article under the terms of the [Creative Commons Attribution-NonCommercial-NoDerivs License](https://creativecommons.org/licenses/by/4.0/), which permits use and distribution in any medium, provided the original work is properly cited, the use is non-commercial and no modifications or adaptations are made.

environments (Manning et al., 2010; Osborn et al., 2023). Flocculation and break-up processes are closely linked to physico-chemical and biological characteristics of primary particles and surrounding waters. Laboratory experiments, field campaigns and numerical simulations have demonstrated that particle properties, suspended sediment concentration (SSC), hydrodynamics, salinity and organic matter can contribute to flocculation and break-up processes at different degrees and at different time scales. Previous studies revealed that SSC is one of the major drivers for flocculation by increasing collision frequency between particles (Pejrup, 1988; M. Ross & Mehta, 1989). However, above a specific value of SSC, suspended sediments fall as a mass instead of independent particles (hindered settling), resulting in lower settling rates. Similarly, turbulence in the flow can have a double effect: at low level, turbulence enhances flocculation, whereas above a threshold value, floc break-up is promoted (Markussen & Andersen, 2014; Pejrup & Mikkelsen, 2010). Salinity and organic matter are recognized to enhance cohesion between particles (Fettweis et al., 2022; Thill et al., 2001). Nevertheless, the influence of salinity on flocculation in estuaries has been called into question in previous studies (Defontaine et al., 2023; Verney et al., 2009).

Knowing that most of the suspended sediments are transported in the form of flocs in estuaries and rivers (Droppo & Ongley, 1994; Eisma, 1986; Guo & He, 2011), flocculation is expected to play a key role in driving cohesive sediment fluxes along the land to seawater system. In the literature, flocculation in freshwater systems (e.g., rivers and lakes) was generally studied separately from flocculation in estuarine and marine systems (Nghiem et al., 2022; Osborn et al., 2023). Freshwater flocs have generally been reported to be smaller in size than marine and estuarine flocs in early studies (Droppo & Ongley, 1994). It has long been attributed to limited electro-chemical flocculation due to the absence of salt. Nevertheless, recent studies have shown that floc sizes can be of the same order of magnitude in the entire riverine/estuarine system (Guo & He, 2011). Major drivers and time scales involved in flocculation processes in rivers generally differ from estuaries. Biological factors and suspended sediment concentration have been reported to be two of the major drivers of freshwater flocculation with strong seasonal variation (Lee et al., 2019; Osborn et al., 2023; Walch et al., 2022), while in the estuary hydrodynamics is expected to play a more significant role. Suspended sediment concentration and turbulent shear are commonly considered to be controlling factors of estuarine flocculation on very short time scales (less than 6 hr) (Pejrup & Mikkelsen, 2010; Van der Lee, 1998; Verney et al., 2009). Studies considering the entire riverine/estuarine system are scarce (Guo & He, 2011; Le et al., 2020) and the freshwater floc generation, growth, breakup and transport into downstream estuaries are still largely unknown. Studying the flocculation dynamics in fresh and saline waters would contribute to a better understanding of the evolution of the flocs' characteristics as well as the sediment trapping capacity within the entire riverine/estuarine continuum.

Gaining insights into cohesive sediment transport requires high-quality in situ estuarine floc data, which is generally both expensive and logistically difficult to collect. Contrary to laboratory experiments, field surveys may face complications due to the inherent complexity of natural environments, where numerous drivers vary simultaneously, making the interpretation of floc behavior non trivial. With this in mind, field campaigns have been carried out in the Garonne-Gironde fluvial-estuarine system with an innovative instrument known as System for the Characterization of Aggregates and Flocs (SCAF). In this study, we aim to answer the following question: What is the response of the cohesive sediment settling velocity to two environmental conditions along the same land-to-ocean continuum? The role of different hydrodynamic and environmental factors such as suspended sediment concentration, turbulence, salinity and organic content is discussed, and variations in the settling velocity along the water column are also analyzed.

2. Study Area

2.1. Gironde Estuary—GE

The Gironde Estuary (GE) is a well-mixed to partially mixed funnel-shaped estuary subject to a semi-diurnal macrotidal forcing, located along the French Atlantic coast (Figure 1). The estuary is 75-km long from the mouth of the estuary to the confluence of the two tributaries: the Garonne and Dordogne Tidal Rivers. The combined average Garonne and Dordogne Rivers discharge is approximately 760 m³/s, with lower daily values of 50 m³/s during the dry season (summer to fall) and higher values of 5,000 m³/s during extreme flood events. The saline intrusion is typically limited to the confluence of the tidal rivers, except under moderate to low river flow conditions (below 400 m³/s) (Van Maanen & Sottolichio, 2018). The subtidal density stratification inside the estuary varies according to two time scales: (a) the fortnightly tidal cycle, from well-mixed during spring tide to

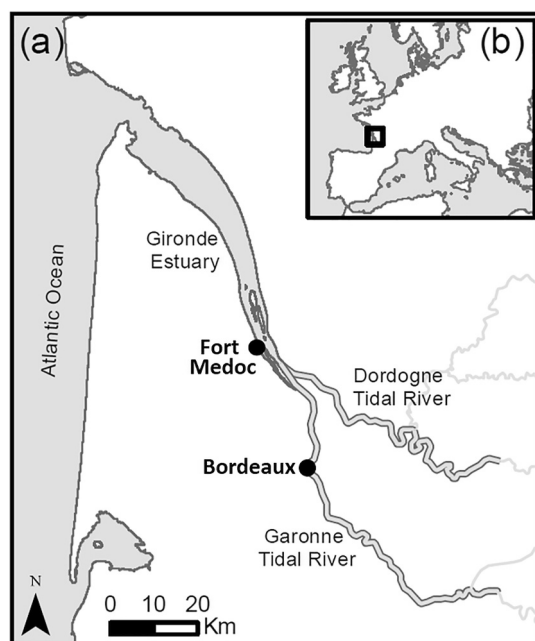


Figure 1. Location map of the Gironde-Garonne fluvial-estuarine system. Black dots represent the observation stations.

partially mixed during neap tide; (b) the seasons, with stronger stratification during high river discharge periods (winter and spring) and lower stratification during dry seasons (summer and fall) (Allen et al., 1980). The GE is characterized by a high level of turbidity, with SSC that may reach up to 1 g per liter in the ETM (Jalón-Rojas et al., 2015; Sottolichio et al., 2011). Fine-grained sediments from fluvial sources accumulate in the lower estuary around Fort Médoc where a permanent ETM is observed, generally attributed to local resuspension of sediments (Sottolichio & Castaing, 1999).

2.2. Garonne Tidal River—GTR

The Garonne Tidal River (GTR) is defined as the portion of the Garonne River extending from its confluence with the Dordogne River (head of the Gironde Estuary) to the upper limit of the tidal propagation (Figure 1). The tidal influence stretches out over 100 km (Jalón-Rojas et al., 2018). During its propagation from the mouth, the tidal wave amplifies and distorts to reach its maximum amplitude in the tidal rivers. It is asymmetrical, with a shorter flood duration (e.g., 4hr at Bordeaux) and stronger flood current intensity (Bonneton et al., 2015; L. Ross & Sottolichio, 2016), generating a second, larger ETM by tidal pumping mechanism (Van Maanen & Sottolichio, 2018). Under low river discharge conditions, this ETM moves upstream into the tidal rivers, its core locates around Bordeaux in the GTR, with maximum SSC reaching up to 10 g/L in the ETM (Defontaine et al., 2023; Jalón-Rojas et al., 2015; Sottolichio et al., 2011). The residence time of particles inside the ETM has

been evaluated to range from 1 to 2 years (Jouanneau & Latouche, 1981). Along the estuary, surface particulate organic carbon (POC) is mainly refractory, of 98% terrestrial origin, and 2% phytoplankton origin, respectively (Etcheber et al., 2007; Savoye et al., 2012). Suspended sediments in the ETM are characterized by low POC content, ca. 1.5%, in any season and a low lability of this POC (Etcheber et al., 2007).

3. Materials and Methods

Field surveys were conducted at two selected sites 50 km apart representing respectively tidal river and estuarine environments: Bordeaux (GTR) and Fort Médoc (GE) (Figure 1), on 26th and 29th September 2022. During these surveys, the tidal range was 5 and 4.6 m (i.e., spring tide) and river flow was 82 m³/s and 132 m³/s (i.e., dry season) at Bordeaux (GTR) and Fort Médoc (GE), respectively. Both locations exhibited the presence of an ETM during these surveys. At each station, an identical protocol was employed to measure bottom and surface SSC, sediment settling velocity, flocculation ability, and organic matter properties (POC and C/N). Additionally, full vertical profiles of velocity, turbidity, salinity, and temperature were recorded in the water column.

3.1. Settling Velocity and Flocculation Ability Measurements

Many techniques are available to assess in situ settling velocity, such as video-based techniques, for example, (Manning & Dyer, 2007; Osborn et al., 2021). Despite their numerous advantages, the specificity of the Gironde Estuary and Garonne Tidal River (e.g., SSC often around 10 g/L) led us to disregard any imaging system. In our recent study presented in Defontaine et al. (2023), we have demonstrated that the recently patented System for the Characterization of Aggregates and Floccs (SCAF) offers a highly suitable and advantageous approach for quasi in situ measurements of settling velocities of fine suspended sediments in highly turbid waters. Therefore, in the present study, we have followed a similar protocol to the one presented in Defontaine et al. (2023).

The SCAF instrument is an optical settling column that estimates the settling velocity and the flocculation ability of cohesive sediments based on the time and depth variation of optical absorbance. It is equipped with 16 infra-red optical emitters and diametrically opposed photo-sensors distributed along the 20 cm long glass tube. The eight upper sensors provide an estimate of particle settling velocity in quiescent waters $W_{s,upper}$ while the eight lower sensors provide an estimate of the particle settling velocity after flocculation $W_{s,lower}$. A flocculation index is then computed as: $FI = (W_{s,lower} - W_{s,upper}) / W_{s,upper}$. A flocculation index equal to zero indicates a non-cohesive behavior, while higher values imply a higher flocculation ability of particles in quiescent waters. For high

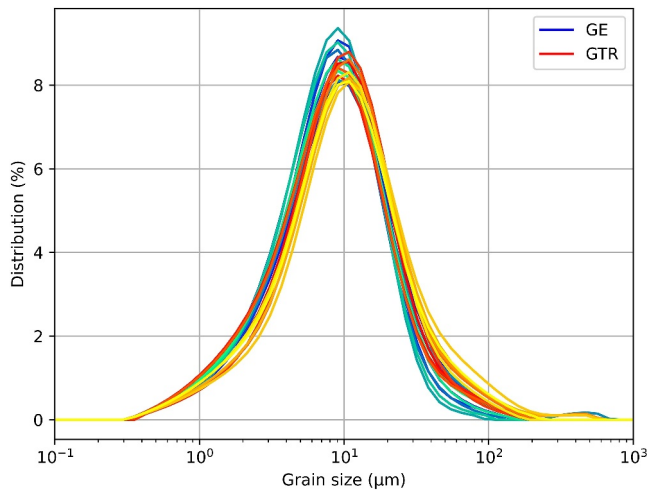


Figure 2. Particle size distribution of the dispersed particles (i.e., after stirring and sonication of the samples) collected at both sites along the tidal cycle (from blue to green for GE and from red to yellow for GTR).

sites were solely composed of fine-grained cohesive sediment; the median diameter of dispersed particles varied between 7.2 and 9.9 μm , with D_{10} values ranging from 1.9 to 2.6 μm and D_{90} values ranging from 18.1 to 37.3 μm (Figure 2).

3.2. Hydro-Physico Parameters Measurements

Settling velocity measurements have been complemented by measurements of flow velocity, turbidity, temperature and salinity profiles. A Workhorse Sentinel 600 KHz ADCP was deployed down looking to collect velocity profiles every 10 min at 8 Hz during the whole tidal cycle. Vertical profiles of salinity, temperature and turbidity were performed every 30 min with an NKE MPx multiparameter probe. Water samples were collected every hour to estimate precisely SSC by filtration from the same samples used for settling velocity estimates and to support the laboratory calibration of the turbidity probe only used for turbidity profiles conversion presented Figures 4e and 4f.

Water samples were filtered through pre-combusted and pre-weighted GF/F filters (47 mm diameter) for suspended particulate matter (SPM) and elemental analysis (both parameters were analyzed on the same filter). Filters were dried at 60°C, then stored in a desiccator. Prior to analysis, filters for elemental analyses were decarbonated by contact with HCl vapor (8 hr) following Lorrain et al. (2003). One or two punches (11 mm diameter) from each filter were analyzed for particulate organic carbon (POC) and particulate organic nitrogen (PON) using an elemental analyzer (Thermo Finnigan Flash EA 1112 analyzer). Organic material characteristics (POC:SSC (%) and C/N) measured during our field experimentation were in good agreement with what had been observed in previous studies (Savoie et al., 2012), to know POC:SSC values below 2% and C/N ratio around 9 (Figure 3). Those values are relatively constant in time and space, and they indicate a very low content of refractory organic material.

3.3. Turbulence and Stratification

To characterize the turbulence inside the water column and assess the influence of density stratification on the turbulence, we estimated the turbulent shear G and the Richardson number Ri inside the water column.

Following Pejrup and Mikkelsen (2010), the turbulent shear has been computed as the root mean square velocity gradient G :

$$G = \sqrt{\frac{u_*^3 (1 - z/H)}{\nu \kappa z}}, \quad (1)$$

concentration suspension (i.e., under hindered settling regime), only the settling velocity of the front was estimated with the five central sensors, and consequently no distribution of velocity or flocculation index was computed. For further details on the SCAF functioning, the reader may refer to Wendling (2015), Wendling et al. (2015), and Gratiot et al. (2015). This device has been utilized successfully to assess the settling velocity and flocculation in different environments (Defontaine et al., 2023; Le et al., 2020; Legout et al., 2018). However, it is worth noting that the SCAF does not allow for the measurement of particle size or density, which can be considered a limitation.

At each dock station, water samples were collected with a Niskin bottle five times during the entire semi-diurnal tidal cycle, both at the surface and near the bottom of the water column. Immediately after each sampling, 180 mL of subsamples were directly introduced into two copies of the SCAF device. The suspended sediments settled in the column during 1h30 as suggested in Defontaine et al. (2023), limiting the number of samples per tidal cycle to five. After settling, a grain size analysis was performed on the sediment from the settling experiment. The analysis was made in the laboratory using a Malvern laser-diffraction instrument (after stirring and sonication of the samples). The size distribution analysis revealed that sediments from both

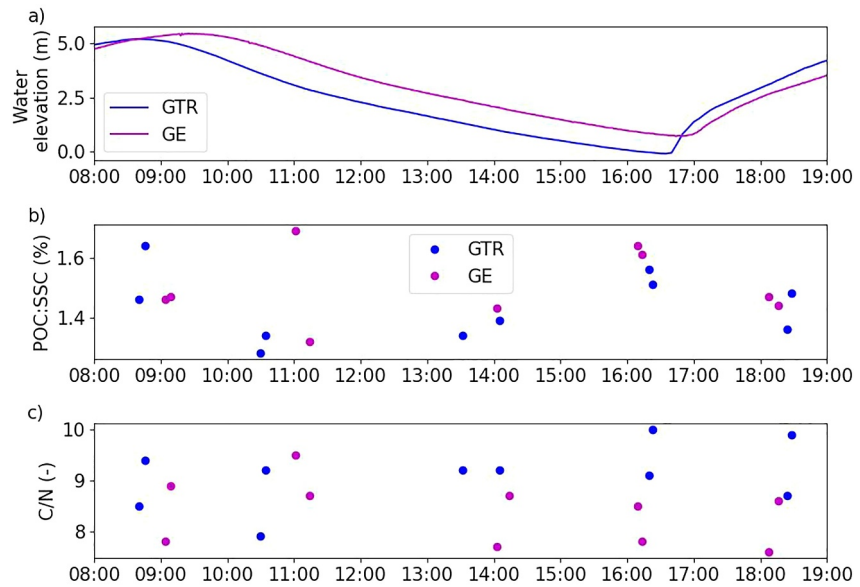


Figure 3. Time evolution of: (a) water elevation (m) (b) POC:SSC (%) and (c) C/N inside the Gironde Estuary (GE) and Garonne Tidal River (GTR).

where u_* is the friction velocity, H is the water depth, ν is the kinematic viscosity, and κ is the Von Karman's constant (~ 0.41). The friction velocity u_* was computed by using the velocity profiles from ADCP measurements with the hypothesis of the logarithmic inner law. Estimation of u_* were made only with profiles of at least 8 data points and if the fit with the log profile has an acceptable correlation coefficient $r^2 > 0.6$. These criteria discard mostly profile during slack time when current reversal induced a deviation from the log profile ($r^2 < 0.6$) and velocity profiles at low tide time (with less than 8 data points). It is worth underlining that uncertainties in u_* computation may be high, as the ADCP may face difficulties in accurately measuring flow velocity close to the bed due to the presence of fluid mud.

The stability of the density stratification has been quantified using the non-dimensional Richardson number:

$$R_i = -\frac{g}{\rho_0} \frac{\partial \rho / \partial z}{(\partial u / \partial z)^2} \quad (2)$$

with ρ_0 being the depth-averaged density. The density has been calculated accounting for the effect of suspended sediment concentration. The water column is considered stable when the buoyancy forces overcome and suppress turbulent mixing (high values of R_i). Otherwise, turbulent mixing is supposed to be sufficient to breakdown the stratification. Typically, a threshold value of 0.25 is used to distinguish a stable stratified water column from an unstable well-mixed water column.

4. Results

This section presents the observations of sediment settling dynamics in the Garonne Tidal River (GTR) and the Gironde Estuary (GE) during one tidal cycle. Settling velocity distributions are presented in relation to local hydrodynamics at both stations (Figure 4). In this section, the term settling velocity will refer to the median settling velocity of a population of flocs in a water sample.

4.1. Sediment Dynamics in the GTR

In the GTR, the flood tide is shorter than the ebb tide leading to strong flood currents and resuspension. During the 4 hr of rising tide, the current velocity exceeded 1 m/s, and the resuspension led to SSC of up to 34 g/L about 70 cm above the bed. Such high concentrations resulted in a hindered settling where the settling occurred by mass,

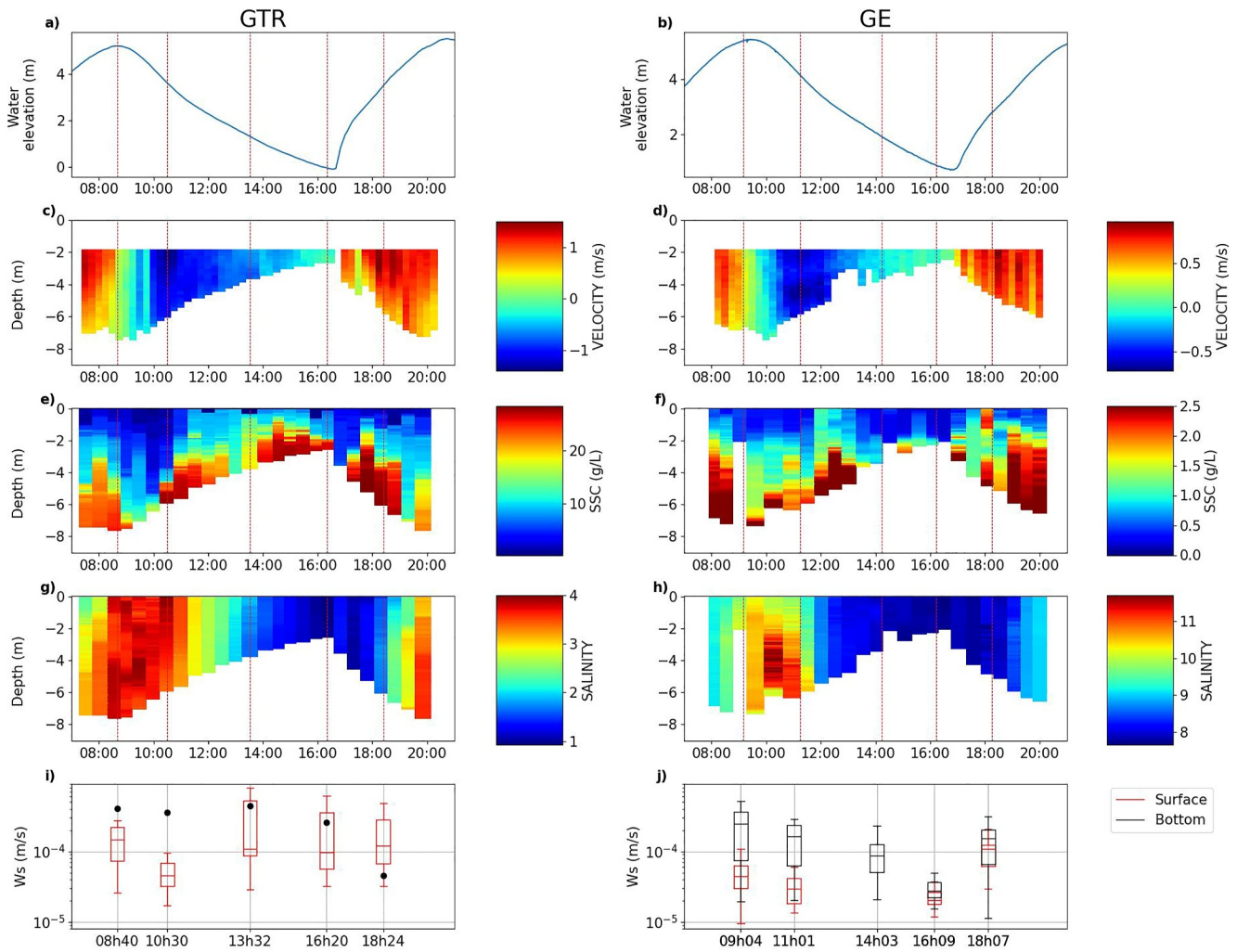


Figure 4. Time series of (a) and (b) water elevation in meters, (c) and (d) velocity profiles in meters per second, (e) and (f) suspended sediment concentration in grams per liter, (g) and (h) salinity, and (i) and (j) settling velocity distribution of suspended sediments from surface and bottom waters in meters per second. When concentration is too high (i.e., under hindered settling regime), no distribution of velocity can be estimated only the settling velocity of the front was estimated (black dots on subplot i). Data collected in the GTR on September 26th and in the GE on September 29th.

resulting in a relatively low settling velocity of $4.5 \cdot 10^{-5}$ m/s (at mid flood—18h30). Conversely, at the surface, SSC was lower (2.76 g/L) and the settling velocity was one order of magnitude higher ($1.2 \cdot 10^{-4}$ m/s).

At high water (08h40), the current began to slow down and SSC decreased. The settling velocity of surface flocs remained at $1.4 \cdot 10^{-4}$ m/s, whereas the settling velocity of suspended sediments close to the bed increased to $4.1 \cdot 10^{-4}$ m/s. During high water slack (i.e., minimum of current intensity—09h00), the salinity was homogeneous along the water column and it reached a maximum value of 4 g/L, while low SSC was observed due to particle deposition. Thereafter, in surface water, only smaller particles stayed in suspension leading to a narrow distribution of settling velocity and a median value of $4.5 \cdot 10^{-5}$ m/s. Close to the bed, the SSC diminished but stayed above 10 g/L and the settling velocity kept almost constant. Afterward, the outflow accelerated, generating resuspension on the bed which spread sediment along the water column. Around 13h00, the current slowed down and it was no longer able to resuspend sediment. But the remaining sediments were widely spread along the water column. Surface waters sediment settling velocity increased to $1.1 \cdot 10^{-4}$ m/s and the distribution became broader. At 14h00, the salt water was flushed out and fresh water arrived with a highly concentrated sediment layer. During the last 2 hr of the falling tide, in spite of the low current velocity, the suspended sediment concentration was very high, due to a highly concentrated sediment layer advecting downward with the flow. On the surface, SSC reached 10 g/L due to the reduction of the depth of the water column. The settling velocity of sediments from both surface

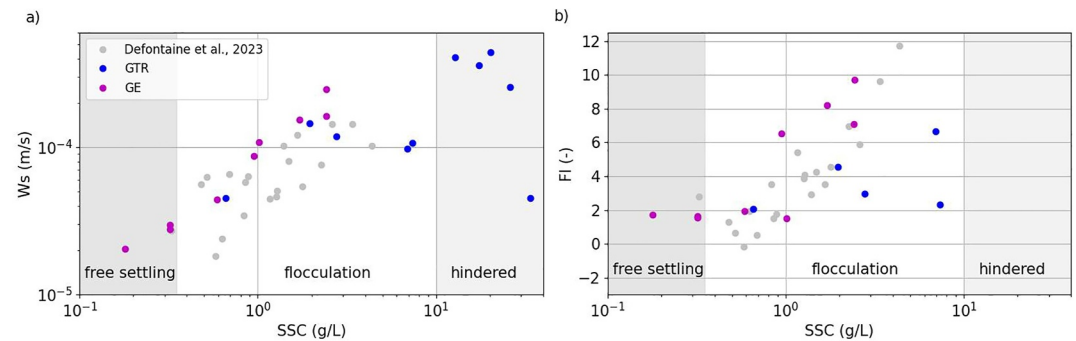


Figure 5. (a) variation of the settling velocity (in meters per second) regarding SSC (in grams per liter), (b) variation of the flocculation index (FI) as a function of SSC (in grams per liter) for both stations. Data of surface water samples collected in the GTR in 2021 from Defontaine et al. (2023) is represented in gray.

and bottom waters stayed relatively constant. On average, the settling velocity in the GTR was of $2 \cdot 10^{-4}$ m/s, with values up to $4.4 \cdot 10^{-4}$ m/s close to the bed.

Figure 5 represents the observed settling velocity and flocculation index in relation to SSC in the tidal river and estuarine stations. Observations from Defontaine et al. (2023) in the tidal river are also depicted (in gray). Three settling regimes can be observed: (a) the free settling regime is observed for low SSC, allowing the particles to settle quasi independently from each other (i.e., no or weak flocculation); (b) flocculation regime occurs at intermediate level of SSC (from hundreds of milligrams to few grams per liter); at this regime interactions between individual particles are enhanced and therefore flocculation mechanisms are promoted, resulting in an increased settling velocity; (c) the hindered settling regime takes place at extremely high SSC (above several grams per liter) when particle interactions and collisions induce a reduced group settling. It worth noting that the definition of the free settling regime was based on the small values of the flocculation index. However only few data were collected at low concentration, thus this limit should be considered with caution. The upper limit that segregates flocculation from hindered settling regime has been defined as the upper concentration above which a settling front has been observed. In the GTR, sediments from bottom waters were always under hindered settling due to very high SSC (above 10 g/L), whereas sediments in surface waters were under flocculation regime (Figure 5). This result highlights the dominant role of SPM concentration in the flocculation process, hence on the settling velocity.

4.2. Sediment Dynamics in the GE

In the estuarine station, currents were lower than in the Tidal River due to the wider estuary cross-sectional area (Figure 4d). In particular, the flood currents were lower as the tidal asymmetry is less pronounced there (flood phase of 5h20) in the GE than in the GTR (Figure 5). Consequently, SSC in the GE was significantly lower (one order of magnitude) than in the GTR, with no fluid mud layer on the bed (Figure 4f).

At the beginning of the flood (18h00), the current increased quickly and generated resuspension along the whole water column (Figure 4d). The settling velocity distributions of suspended sediments from surface and bottom waters were similar, even though the distribution for sediments from surface waters was slightly narrower. The median settling velocity of sediments from surface and bottom waters was $1.1 \cdot 10^{-4}$ and $1.5 \cdot 10^{-4}$ m/s, respectively (Figure 4j). At the end of the flood (09h04), the current intensity decreased, limiting the resuspension to the lower half of the water column. A vertical stratification was observed in the SSC profiles with a bottom value of 2.42 g/L and a surface value of 0.59 g/L (Figure 4f). Settling velocity distributions were strongly dissimilar between the bottom and surface waters, suggesting a different distribution of particle size. Near the bottom, settling velocity and therefore particle size exhibited a wide distribution and a median value of $2.74 \cdot 10^{-4}$ m/s, whereas, at the surface, the distribution was narrow with a lower median value of $4.4 \cdot 10^{-5}$ m/s. This difference between the two distributions seems to indicate that bigger particles (previously resuspended by strong flood currents) settled down to the lower part of the water column.

At high water slack time (10h00), current velocity is incapable of resuspending sediments from the bed or maintaining them in suspension. Deposition occurred and led to low SSC in the whole water column. Salinity

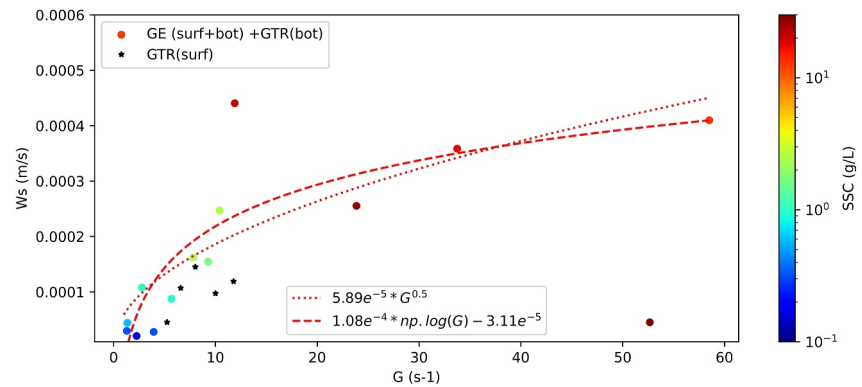


Figure 6. Settling velocity data as function of turbulent shear and suspended sediment concentration for both sites. Data collected in surface waters in the GTR in 2022 are indicated with black stars.

reached its maximum value of 12 in the lower half of the water column, and a vertical stratification was observed. During ebb tide, current intensity was slightly lower than during flood tide and decreased rapidly. No strong resuspension period was observed and sediments were progressively deposited on the bed. Consequently, settling velocities of sediments from surface and bottom waters decreased progressively and their distributions became narrower. This trend continued until the ebb slack stage, when settling velocities reached their minimum values.

In the GE, the SSC stayed below a moderate level, preventing sediments to reach the hindered settling regime. Sediments mostly remained in the flocculation regime where the flocculation ability of sediments (FI) and thus the settling velocities linearly increased with SSC (Figure 5). However, below a very low level of SSC (i.e., during ebb tide), sediments were under a free settling regime where FI and W_s remained very low.

5. Discussion

In this section, data from a former study by Defontaine et al. (2023) have been added in the figures to be discussed (gray dots), as previously done in Figure 5. These data have been collected in surface waters of the GTR with a similar protocol along 6 tidal cycles (spring and neap) from May to September 2021.

5.1. Influence of Turbulent Shear

It is widely accepted that water turbulent shear significantly influences the flocculation process and, consequently, the settling velocity of flocs in a turbulent flow. A low to moderate level of turbulence enhances flocculation through a higher collision probability, whereas at a higher current velocity and a higher turbulence level, the flocs are broken into smaller constituents (Eisma, 1986). Numerous studies have attempted to relate the median velocity to the turbulent shear parameter G (Manning & Dyer, 1999; Winterwerp, 1998), although only a few of these analyses were conducted with in situ data (Pejrup & Mikkelsen, 2010).

In order to investigate the effects of turbulence on the settling velocity in the Gironde-Garonne system, the settling velocity data for both sites were plotted against the turbulent shear parameter G (Figure 6). In the entire data set, G varied between 0.1 s^{-1} and 58 s^{-1} throughout the water column, depending on the tidal phase. Similar ranges of G values have also been observed in other estuaries (Pejrup & Mikkelsen, 2010; Van der Lee, 1998). As the current velocity was stronger in the Garonne Tidal River than in the Gironde Estuary, the range of values for G were also higher. Along the vertical, G was generally one order of magnitude lower on the surface. Figure 6 highlights that the settling velocity increased with increasing G and a maximum settling velocity is reached around 10 s^{-1} , above which the settling velocity seemed to decrease with increasing turbulence. Such observation are generally attributed to the fact that low to moderate mixing enhances flocculation hence increasing w_s , while a higher level of turbulence exceeded the strength of cohesion between constituents of flocs. Similar trends have been observed in the literature, for example, Pejrup and Mikkelsen (2010) has shown that in the RømøDyb channel the maximum settling velocity is obtained for a value of G at 8.5 s^{-1} . However, the threshold value may differ widely from one study site to another. For example, in the Danish Wadden Sea, Markussen and Andersen (2014) found that a threshold value of $G = 4 \text{ s}^{-1}$ was sufficient to break up macroflocs. It should be noted that G varies in correlation

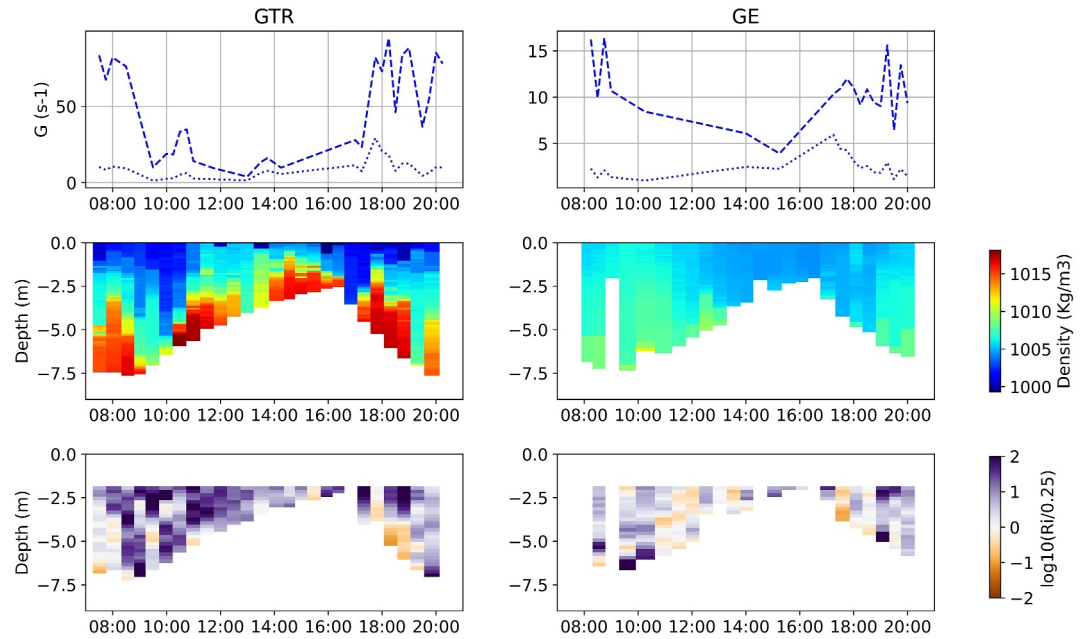


Figure 7. Time series of turbulent shear, water density and stability of the water column during tidal field campaigns in the GTR and GE.

with SSC. This could be explained by the fact that an increasing friction velocity u^* leads to an increase in turbulence as well as an increase in resuspension of bed sediments. Therefore, distinguishing between the effects of both factors, SSC and G , on flocculation processes with in situ data seems to be complex.

The very high concentration in suspended sediments observed at the Bordeaux station may also have a direct impact on the bed-generated turbulence, as it promoted strong density stratification in the water column (Figure 7). This strong stratification seems to be sufficient to stabilize the water column and to damp the turbulence in the upper part of the water column ($Ri \gg 0.25$). In such a configuration, the formulation of the turbulent shear based on the friction velocity is unsuitable to evaluate turbulence close to the surface. Therefore, turbulent shear data from the GTR at the surface should be interpreted with caution (black stars in Figure 6). These data have been discarded of prediction laws interpretation.

5.2. Influence of Water and Sediment Properties

Variations in water properties may induce the modification of a particle's surface characteristics (electrostatic charges), affecting cohesion/repulsion forces between particles and thus the mineral flocculation of fine-grained sediments. Previous studies have shown that the settling velocity of suspended sediments increases when passing from fresh to salty waters (Kim et al., 2016; Portela et al., 2013). In the literature, different threshold values have been found for increasing the cohesion of mineral depending on the studied mineral. For natural sediments, Gibbs et al. (1989) have shown that sediments coagulate upon encountering low salinity (0–2) in the upper estuary, whereas Migniot (1968) has shown that the settling velocity of natural sediments may be increased with salinity until a threshold value of 13. However, other studies drew opposing conclusions with sediments from different estuaries that were insensitive to changes in salinity (Thill et al., 2001; Verney et al., 2009).

Figure 8 shows the variations of settling velocity regarding the salinity. For both study sites, representing different salinity ranges, settling velocity measurements did not reveal a direct influence of salinity. Those results are in

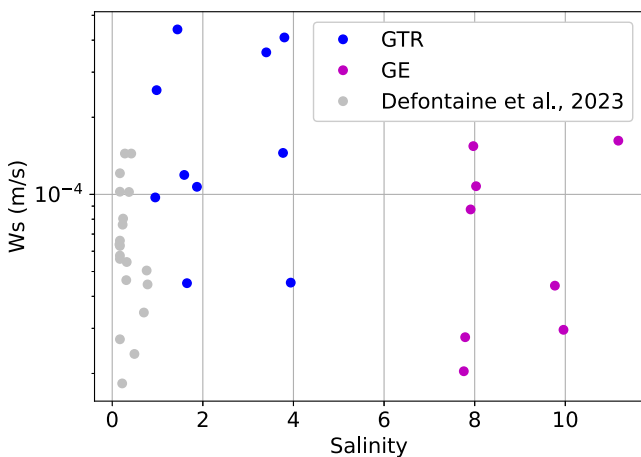


Figure 8. Settling velocity measurements as a function of salinity for both stations. Data collected in the GTR in 2021 presented in Defontaine et al. (2023) has been added in gray for comparison.

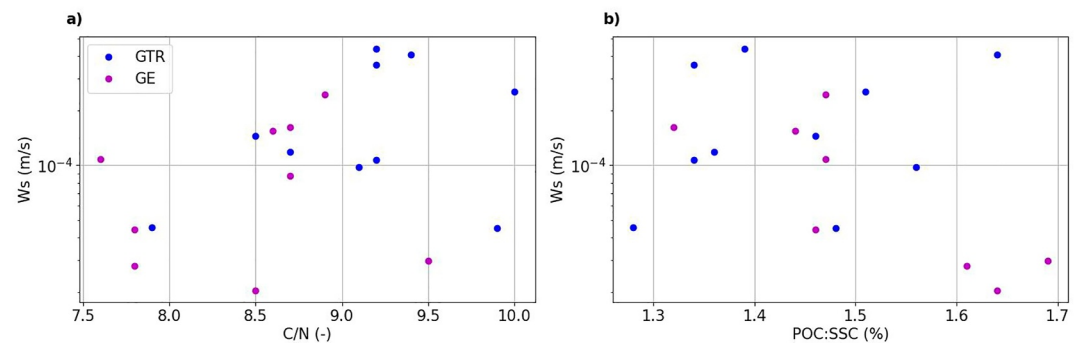


Figure 9. Settling velocity measurements as a function of: (a) the carbon to nitrogen ratio, (b) POC content expressed in % of SSC, at both stations.

line with previous measurements presented in Defontaine et al. (2023) (represented in gray on Figure 8). It can be explained by the fact that, in this hyper turbid system, the effects of salinity on flocculation are lower than other drivers such as SSC or turbulence. As all the drivers vary simultaneously in natural environments, salinity effects can be overcome by the influence of other factors. For example, the maximum salinity is generally reached during high water slack time, which also corresponds to the minimum of SSC and turbulence. In this case, the increased cohesion efficiency due to higher salinity can be counteracted by lower collision probability due to lower SSC and turbulence.

Constituents of natural cohesive sediments may also influence flocculation (Bennett & Hulbert, 2012; Mikes et al., 2004; Milligan & Hill, 1998). Cohesive sediments generally contain organic and chemical compounds including microalgae, polymers or bacteria that affect physico-chemical bonds between sediments. According to previous studies, a large quantity of organic matter favors flocculation by increasing sticking efficiency (Tang & Maggi, 2016), and reinforces particles bounding, making it more resistant to fragmentation (Cross et al., 2013). In addition to the quantity, the origin and lability of the organic matter can also affect the cohesion efficiency (Fettweis et al., 2022). From the current data set (Figure 9), one cannot identify a direct response of w_s against any of the organic content parameters. This could be explained by the very low organic content that was measured in the sediment at both sites (POC:SSC \sim 1.5%), as well as the advanced state of organic matter decomposition (C/N $>$ 8). Etcheber (1986) has shown that, in the Gironde Estuary, the POC content varies seasonally with phytoplankton contributions only outside the turbidity maximum. Liénart et al. (2017) has demonstrated that the phytoplankton contribution to the POM increases along the estuary with salinity and is more important downstream from the ETM (27%) than inside the ETM (2%). In the literature, those very low levels of organic matter in the ETM have been attributed to (a) the lack of light availability, which limits primary production, and (b) the long residence times of suspended sediments allowing for a nearly complete remineralization of the labile organic matter supplied by the river (Abril et al., 1999; Etcheber et al., 2007; Savoye et al., 2012).

It worth noting that even if salinity and organic matter show no direct influence on the settling velocity on muddy sediment it does not mean that these parameters have no influence on the flocculation processes. Such processes could encourage the formation of larger and less dense flocs that would have negligible impacts on the settling velocity. To go further on this issue, information on size and density of flocs would be needed, but this would be outside the scope of the present study.

5.3. Principal Component Analysis (PCA)

A PCA has been carried out with data from GE (surface + bottom) and GTR (bottom) to provide further interpretation of results (Figure 10). Six variables ($n = 6$) has been considered: w_s , SSC, G, salinity, C/N and COP:SSC, for a set of 12 observation ($p = 12$). The data, having different units, were automatically scaled to ensure that their relative influence on the model is independent of the units. Two principle components were extracted, together explaining 79.9% of the information contained in the data set. The global relationship between the variables is determined by SSC, which is correlated to PC1 at 94%. Most of the variables are strongly associated with the first component (PC1): G (83%), C/N (82%), w_s (69%) and Salinity (-92%). Only the POC is highly associated with the second component (92%). The first component seems to underline the fact that highly

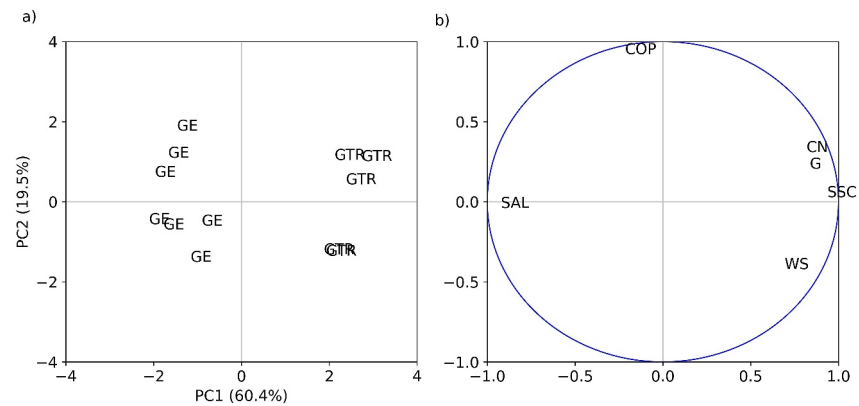


Figure 10. Principal component analysis diagram and correlation circle for w_s , SSC, G, salinity, C/N, COP:SSC for GTR (bottom) and GE (surface + bottom) samples.

concentrated waters occur at period of strong turbulent shear and low salinity, and results in higher sediment settling velocity and more degraded organic matter. The second component seems to indicate that higher content of organic matter and lower the sediment settling velocity, contrary to the idea that organic matter favors bonding between particles which leads to stronger flocculation. PCA diagram reveals that PC1 segregates GTR samples (positive region of PC1) from GE samples (negative region of PC1). The explanation for this is that GE is exposed to more saline waters, lower current intensity (i.e., lower bottom shear stress) and lower SSC, compared to GTR.

5.4. Prediction

Modeling of suspended sediment dynamics requires the accurate prediction of the behavior of flocs in tidal environments. It has long been recognized that SSC is one of the major drivers for the flocculation in such environments (Mehta, 1989; Pejrup, 1988; Verney et al., 2009; Winterwerp, 1998). The data presented in this study specifically supports such a conclusion (Figure 11). The combined GE-GTR curve shows a rising slope characteristic of flocculation behavior. This gentle rising slope compared to other study sites (e.g., Tampa Bay, Severn Estuary, Elbe Estuary) reflects a lower ability to flocculate which can be attributed to low light availability and thus low level and low lability of organic matter. Then settling velocities attain a maximum, forming a plateau due to concentrated suspension, which finally leads to a strong decrease in settling velocity due to hindered settling. This central plateau and subsequent strong decrease in settling velocity occurred at higher SSC than in other study sites (e.g., Tampa Bay, Severn Estuary, Kaw River and Mekong Estuary).

The first exponential increase of the median settling velocity in correlation with the increase in suspended sediment concentration obeys the formula:

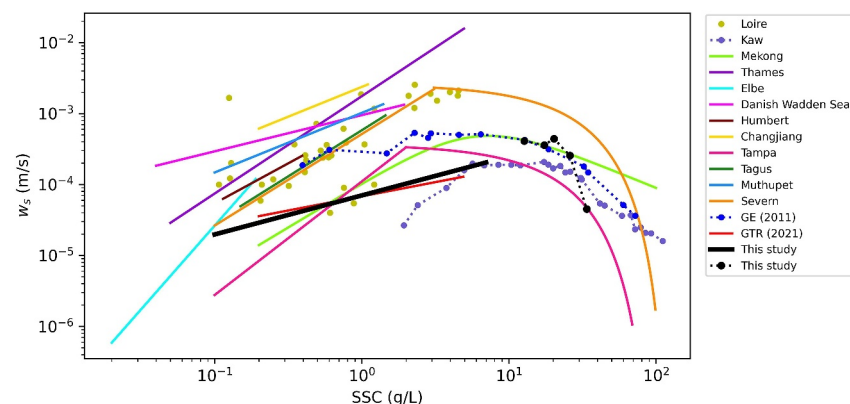


Figure 11. Settling velocity prediction laws as function of SSC from the literature and from this study.

Table 1
Comparison of Different Formulations for the Settling Velocity

Reference	Sediment origin	Field versus lab	Formulation	Instrument
Gratiot and Anthony (2016)	Kaw river mouth	Lab	Data set	Settling column
Personal communication with the GIP Loire estuaries	Loire Estuary	Field	Data set	Owen tube
Gratiot and Anthony (2016)	Mekong Estuary	Lab	$w_s = 0.0045 * \frac{SSC^{1.25}}{(SSC^2 + 6^2)^{1.05}}$	SCAF
Burt (1986)	Thames Estuary	Field	$w_s = 1.341e^{-4} * SSC^{1.372}$ ($r^2 = 0.75$)	Owen tube
Jones and Jago (1996)	Elbe Estuary	Field	$w_s = 5e^{-5} * SSC^{2.37}$ ($r^2 = 0.93$)	Quisset tube
Pejrup (1988)	Danish Wadden Sea	Field	$w_s = 2.798e^{-4} * SSC^{0.51}$ ($r^2 = 0.79$)	Braystoke tube
Pejrup and Mikkelsen (2010)	Humber Estuary	Field	$w_s = 3e^{-4} * SSC^{1.128}$ ($r^2 = 0.89$)	Braystoke tube
Shi et al. (2003)	Changjiang Estuary	Field	$w_s = 2.37e^{-3} * SSC^{0.84}$ ($r^2 < 0.3$)	Rouse profile
van Leussen (1999)	Ems Estuary	Field	$w_s = K * SSC^{2.5}$	RWS settling tube
M. A. Ross (1988)	Tampa Bay	Lab	$w_s = 0.11e^{-3} * SSC^{1.6}$	Settling column
Portela et al. (2013)	Tagus Estuary	Lab	$w_s = 0.37e^{-3} * (1 - 0.01 * SSC)^5$	Settling column
			$w_s = 0.12e^{-3} * SSC^{4.3}$ (S = 0)	
			$w_s = 0.29e^{-3} * SSC^{1.5}$ (S = 5)	
			$w_s = 0.58e^{-3} * SSC^{1.3}$ (S = 10)	
			$w_s = 0.89e^{-3} * SSC^{1.4}$ (S = 15)	
			$w_s = 1.90e^{-3} * SSC^{2.2}$ (S = 30)	
Priya et al. (2015)	Muthupet Estuary	Field	$w_s = 1.02e^{-3} * SSC^{0.84}$	Rouse equation
Mehta (1986)	Severn Estuary	Field	$w_s = 0.513e^{-3} * SSC^{1.29}$	Settling column
			$w_s = 2.6e^{-3} * (1 - 0.008 * SSC)^{4.65}$	
Sottolichio et al. (2011)	Gironde Estuary	Field	Data set	Bergen nautic sediment
Defontaine et al. (2023)	GTR	Field	$w_s = 6.8e^{-5} * SSC^{0.4}$ ($r^2 = 0.41$)	SCAF
This study	GE + GTR	Field	$w_s = 7e^{-5} * SSC^{0.55}$ ($r^2 = 0.65$)	SCAF
Markussen and Andersen (2014)	Danish Wadden Sea	Field	$w_s = -0.026e^{-3} * \log(G) + 0.16e^{-3}$ (Decel. current, $r^2 = 0.76$)	LISST-100C
			$w_s = -0.040e^{-3} * \log(G) + 0.19e^{-3}$ (Accel. current, $r^2 = 0.71$)	
Manning and Dyer (1999)	Tamar estuary	Lab	$w_s = 0.39e^{-3} * G^{-0.24}$ (SSC = 80 mg/L, $r^2 = 0.85$)	Video camera
			$w_s = 0.30e^{-3} * G^{-0.48}$ (SSC = 120 mg/L, $r^2 = 0.84$)	
			$w_s = 0.23e^{-3} * G^{-0.61}$ (SSC = 160 mg/L, $r^2 = 0.86$)	
			$w_s = 0.18e^{-3} * G^{-0.75}$ (SSC = 200 mg/L, $r^2 = 0.90$)	
Manning and Dyer (1999)	Tamar estuary	Lab	$w_s = 0.027 * (SSC * G)^{-0.51}$	Video camera
Priya et al. (2015)	Muthupet Estuary	Field	$w_s = 0.95e^{-3} * SSC^{0.724} * G^{0.47}$	Rouse equation
van Leussen (1994)	Ems Estuary	Field	$w_s = K * SSC^{2.5} * \frac{1 + 0.3 * G}{1 + 0.09 * G^2}$	Settling column
Pejrup and Mikkelsen (2010)	Danish Wadden Sea	Field	$w_s = a * SSC^n * [1 + (k_1 + (k_2 + G^C) * d^{-G})]$	Braystoke settling tube

$$w_s = w * SSC^n, \quad (3)$$

where $w = 7 \cdot 10^{-5}$ and $n = 0.55$ have been determined empirically with the present data set for both sites, with SSC below 10 g/L (Figure 11 and Table 1). The good fit of this regression for both sites indicates that SSC is an adequate explaining parameter ($r^2 = 0.65$). The power exponent (i.e., the flocculation ability) found in this study is very low (i.e., gentle slope), whereas generally the power exponent varies between 0.8 and 3 (Table 1). The power law found in this study also shows a good correlation with data collected in GTR during 6 tidal cycles from May to September 2021 (Defontaine et al., 2023). The regression found here and this proposed in Defontaine

et al. (2023) are very similar and indicate that a unique power law could be used to describe the variation of the settling velocity along the whole Gironde-Garonne system no matter the forcing conditions (Figure 11). Contrast with literature findings, which suggest that settling velocity may vary almost one order of magnitude along a River-Estuary system at the same level of SSC, indicating that no unique power law can be found (Guo & He, 2011; Manning & Schoellhamer, 2013; van Leussen, 1994). For example, in the Yangtze and Ems estuary, the power exponent is greater in the less concentrated area of the system (Guo & He, 2011; van Leussen, 1994). It is worth noting that the data from Sottolichio et al. (2011) collected in the GE do not fit the power law developed in this study. The settling velocity measured in Sottolichio et al. (2011) are an order of magnitude higher than the one presented here. Such disparities between data sets may originate from the different hydrodynamic conditions (ebb vs. flood dominance) faced during the experiments and/or from the different protocols and instruments used to collect data. Nevertheless, when considering data above 10 g/L both studies are consistent.

For the hindered settling regime, most coastal sediment transport studies employed the exact form of Richardson and Zaki (1954) or some related variation (Table 1). Our data set is too scarce above 10 g/L to have a statistically significant correlation to any prediction law. More in situ data needs to be collected to be able to establish an empirical formulation for hindered settling.

As previously discussed, the SSC is not the only factor influencing the settling velocity of suspended particles. Prediction laws have been developed reflecting only the effect of turbulence on the settling velocity (Table 1). Two formulations have been fitted to our data set (Figure 12). Data from surface waters in the GTR have been discarded due to possible improper estimation of G caused by strong vertical density stratification. The formulations using GTR and GE data sets show moderate prediction capacities (in blue in Figure 12). However, if we disregard data for SSC above 30 g/L (in red in Figure 12), prediction abilities are equivalent to those of formulations considering only SSC with the same data set. More complex formulations have been developed to take into account both factors: SSC and turbulence (Table 1). Intuitively, van Leussen (1994) proposed a formulation that add to the still water formulation a term linked to the effect of turbulence on floc growth ($1 + aG$), and a second term owing to floc breakup by turbulence ($1 + bG^2$). More recent studies have developed formulations reflecting the exponential increase/decrease of the settling velocity with the turbulent shear of the flow (Table 1). Such power laws have been tested with our data set. Figure 12 shows that formulations reflecting an exponential increase with the product of SSC and turbulent shear: $w_s \propto (SSC * G)^n$, or a product of an exponential increase of SSC and an exponential increase of turbulent shear: $w_s \propto SSC^n * G^m$ have the best prediction abilities. Such formulations underline the influence of the covariance of G and SSC. These prediction laws show an even better fit to the data when considering only data below 30 g/L (in red on Figure 12), that is, when the SSC is not sufficient to generate a strong decrease in settling velocity ($r^2 = 0.83$). These prediction abilities are also better than the ones obtained with formulation considering SSC only (Equation 3). This demonstrates the major influences of both SSC and G on the settling velocity variations. Nevertheless, more data should be collected over a wider range of G and SSC values to obtain a more reliable prediction law.

The good prediction obtained with SSC and G underlines the influence of local factors on settling velocity. However, due to advection of sediment during the tidal cycle, non-local phenomena may also influence the settling velocity of suspended sediment. Manning and Schoellhamer (2013) identified current velocity 39 min prior to sampling as the best predictor of settling velocity (not SSC nor salinity) in San Francisco Bay. To analyze the relative influence of advection on settling velocity, two close stations should have been selected. In the present study, field sampling stations are outside of sediment advection range.

6. Conclusion

Field surveys were carried out along the Garonne-Gironde fluvial-estuarine system to provide insights into the settling dynamics of muddy sediments exposed to different hydrodynamics and environmental conditions. To estimate the settling velocity of sediments, we deployed SCAF settling columns, which remain a relatively little used and unexplored method in tidal estuaries. Our quasi in situ experimentation confirms the ability of the SCAF instrument to evaluate the settling velocity of suspended sediments at a very high level of SSC of more than 10 g/L (i.e., under hindered settling regime).

In the GTR, pronounced tidal asymmetry and strong current intensity generated high values of SSC and high values of w_s ($4.5 \cdot 10^{-5}$ – $4 \cdot 10^{-4}$ m/s). Suspended sediments were under flocculation regime in surface waters and

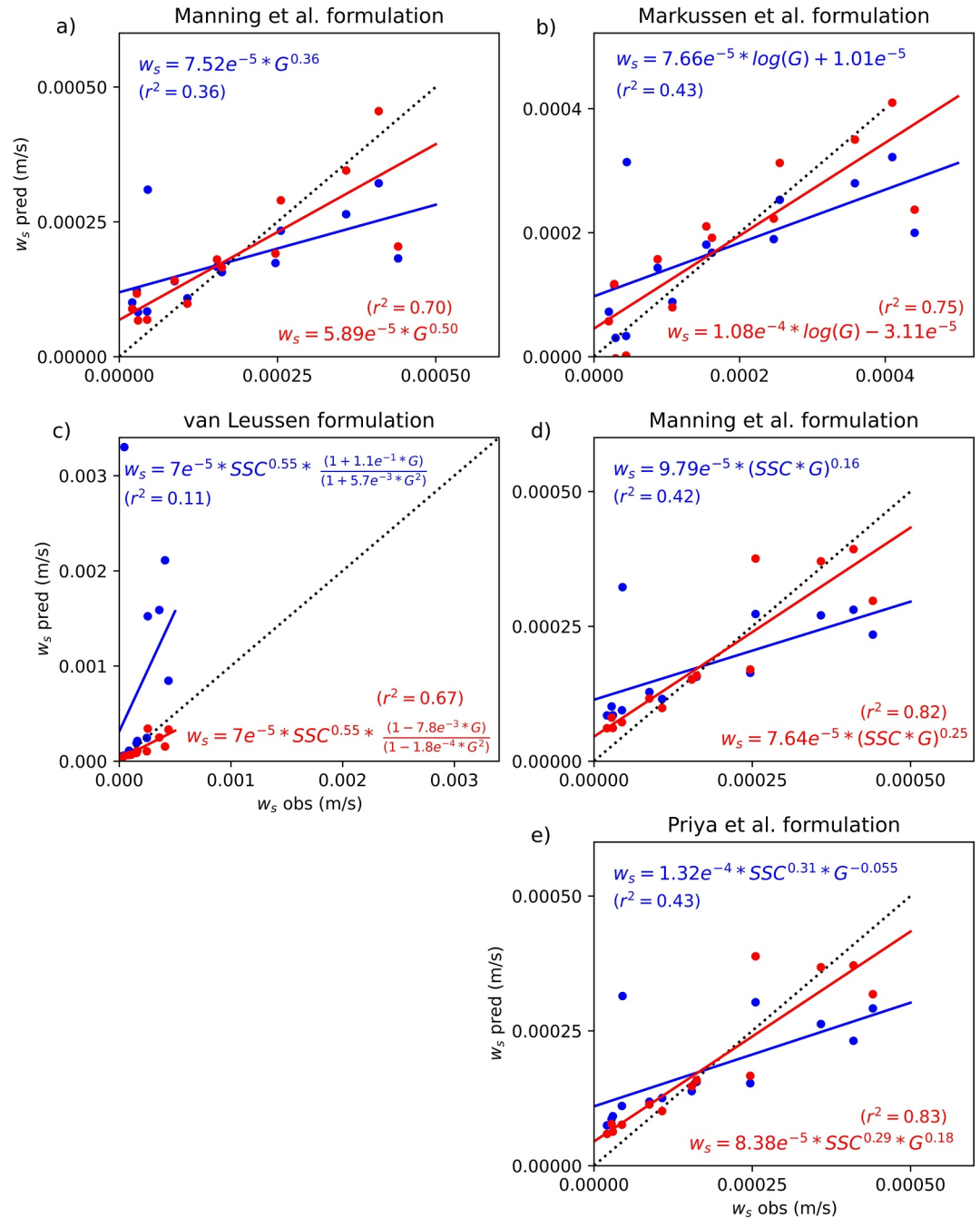


Figure 12. Settling velocity prediction laws as function of G and SSC with data from GE (surface and bottom) and GTR (bottom) in blue. In red, only the data under 30 g/L have been considered for the prediction laws.

under hindered settling regime in bottom waters. Close to the bed, w_s was mostly constant along the tidal cycle, whereas in surface waters w_s was affected by the cycle of erosion, deposition and resuspension. On the other hand, in the GE, current intensity was weaker and SSC was one order of magnitude lower than in the GTR. Settling velocities were also lower ($2 \cdot 10^{-5}$ – $2.7 \cdot 10^{-4} \text{ m/s}$) compared to the ones observed in the GTR, but exhibited more variation. Suspended sediments were mostly under flocculation regime; however, in surface waters during ebb slack time, suspended sediment fell under free settling regime.

The processes responsible for the occurrence of differences in settling velocity between estuarine and tidal riverine environments have been examined using the present data set. In both ETM regions the settling velocity

was mainly influenced by the suspended sediment concentration. Threshold values of SSC allow us to distinguish between the three commonly observed settling regimes. Compared to SSC, the turbulence appeared to be a control parameter of secondary importance whose effects are difficult to distinguish from those of SSC. A new series of field measurements would be necessary to be able to properly evaluate the relative impact of turbulence on the settling of suspended sediments in such turbid and stratified environments. Measurements of w_s associated to salinity and organic content measurements do not reveal any easily identifiable trend. It has been hypothesized that salinity influence on w_s may be counteracted by the effects of SSC and G , as they all vary simultaneously. The lack of light availability in such hyper-turbid systems was probably responsible for the very low content of organic matter and, consequently, its negligible influence on w_s .

On the contrary to other systems around the world, common prediction laws have been successfully fitted to data from both riverine and estuarine waters. The formulation reflecting an exponential increase of w_s with a product of an exponential increase of SSC and an exponential increase of turbulent shear: $w_s \propto SSC^n * G^m$ have shown the best prediction abilities.

Data Availability Statement

Field data presented in this study is publicly available on the open scientific data repository SEANOE (SEA scieNtific Open data Edition) dedicated to marine sciences field at <https://doi.org/10.17882/98376>.

Acknowledgments

This study was supported by the EMPHASE project (ANR-FRQ). The authors acknowledge Marie-Claire Perello for the granulometric analysis, Nathalie Labourdette for the CHN analysis and they are grateful to Armelle Brouquier, Olivier Burvingt, the port of Bordeaux and the city of Fort Médoc for their support during fieldwork. Authors are grateful to the GIP Loire Estuaire for providing settling velocity data collected in the Loire Estuary.

References

- Abril, G., Etcheber, H., Le Hir, P., Bassoullet, P., Boutier, B., & Frankignoulle, M. (1999). Oxidic/anoxic oscillations and organic carbon mineralization in an estuarine maximum turbidity zone (The Gironde, France). *Limnology & Oceanography*, 44(5), 1304–1315. <https://doi.org/10.4319/lo.1999.44.5.1304>
- Allen, G. P., Salomon, J., Bassoullet, P., Du Penhoat, Y., & De Grandpre, C. (1980). Effects of tides on mixing and suspended sediment transport in macrotidal estuaries. *Sedimentary Geology*, 26(1–3), 69–90. [https://doi.org/10.1016/0037-0738\(80\)90006-8](https://doi.org/10.1016/0037-0738(80)90006-8)
- Bennett, R., & Hulbert, M. (2012). Clay microstructure.
- Bonneton, P., Bonneton, N., Parisot, J.-P., & Castelle, B. (2015). Tidal bore dynamics in funnel-shaped estuaries. *Journal of Geophysical Research: Oceans*, 120(2), 923–941. <https://doi.org/10.1002/2014jc010267>
- Burt, N. T. (1986). Field settling velocities of estuary muds. *Estuarine Cohesive Sediment Dynamics*, 14, 126–150. https://doi.org/10.1007/978-1-4612-4936-8_7
- Cross, J., Nimmo-Smith, W. A. M., Torres, R., & Hosegood, P. J. (2013). Biological controls on resuspension and the relationship between particle size and the Kolmogorov length scale in a shallow coastal sea. *Marine Geology*, 343, 29–38. <https://doi.org/10.1016/j.margeo.2013.06.014>
- Defontaine, S., Jalon-Rojas, I., Sottolichio, A., Gratiot, N., & Legout, C. (2023). Settling dynamics of cohesive sediments in a highly turbid tidal river. *Marine Geology*, 457, 106995. <https://doi.org/10.1016/j.margeo.2023.106995>
- Droppo, I., & Ongley, E. (1994). Flocculation of suspended sediment in rivers of southeastern Canada. *Water Research*, 28(8), 1799–1809. [https://doi.org/10.1016/0043-1354\(94\)90253-4](https://doi.org/10.1016/0043-1354(94)90253-4)
- Eisma, D. (1986). Flocculation and de-flocculation of suspended matter in estuaries. *Netherlands Journal of Sea Research*, 20(2–3), 183–199. [https://doi.org/10.1016/0077-7579\(86\)90041-4](https://doi.org/10.1016/0077-7579(86)90041-4)
- Etcheber, H. (1986). *Biogéochimie de la matière organique en milieu estuarien: comportement bilan, propriétés, cas de la gironde*. Institut de géologie du bassin d'Aquitaine.
- Etcheber, H., Taillez, A., Abril, G., Garnier, J., Servais, P., Moatar, F., & Commarieu, M.-V. (2007). Particulate organic carbon in the estuarine turbidity maxima of the Gironde, Loire and Seine estuaries: Origin and lability. *Hydrobiologia*, 588(1), 245–259. <https://doi.org/10.1007/s10750-007-0667-9>
- Fettweis, M., Schartau, M., Desmit, X., Lee, B. J., Terseleer, N., Van der Zande, D., et al. (2022). Organic matter composition of biomineral flocs and its influence on suspended particulate matter dynamics along a nearshore to offshore transect. *Journal of Geophysical Research: Biogeosciences*, 127(1), e2021JG006332. <https://doi.org/10.1029/2021jg006332>
- Fox, J., Ford, W., Strom, K., Villarini, G., & Meehan, M. (2014). Benthic control upon the morphology of transported fine sediments in a low-gradient stream. *Hydrological Processes*, 28(11), 3776–3788. <https://doi.org/10.1002/hyp.9928>
- Geyer, W. R., & Ralston, D. (2018). A mobile pool of contaminated sediment in the Penobscot Estuary, Maine, USA. *Science of the Total Environment*, 612, 694–707. <https://doi.org/10.1016/j.scitotenv.2017.07.195>
- Gibbs, R., Tshudy, D., Konwar, L., & Martin, J. M. (1989). Coagulation and transport of sediments in the Gironde Estuary. *Sedimentology*, 36(6), 987–999. <https://doi.org/10.1111/j.1365-3091.1989.tb01536.x>
- Gratiot, N., & Anthony, E. J. (2016). Role of flocculation and settling processes in development of the mangrove-colonized, amazon-influenced mud-bank coast of South America. *Marine Geology*, 373, 1–10. <https://doi.org/10.1016/j.margeo.2015.12.013>
- Gratiot, N., Coulaud, C., Legout, C., Mercier, B., Mora, H., & Wendling, V. (2015). Unit for measuring the falling speed of particles in suspension in a fluid and device comprising at least one measuring unit and one automatic sampler. Patent-Publication Number WO2015055963, A, 1.
- Guo, L., & He, Q. (2011). Freshwater flocculation of suspended sediments in the Yangtze River. *China*, 61(2–3), 371–386. <https://doi.org/10.1007/s10236-011-0391-x>
- Hassard, F., Gwyther, C. L., Farkas, K., Andrews, A., Jones, V., Cox, B., et al. (2016). Abundance and distribution of enteric bacteria and viruses in coastal and estuarine sediments—A review. *Frontiers in Microbiology*, 7, 1692. <https://doi.org/10.3389/fmicb.2016.01692>
- Jalón-Rojas, I., Schmidt, S., & Sottolichio, A. (2015). Turbidity in the fluvial Gironde Estuary (southwest France) based on 10-year continuous monitoring: Sensitivity to hydrological conditions. *Hydrology and Earth System Sciences*, 19(6), 2805–2819. <https://doi.org/10.5194/hess-19-2805-2015>

- Jalón-Rojas, I., Sottolichio, A., Hanquiez, V., Fort, A., & Schmidt, S. (2018). To what extent multidecadal changes in morphology and fluvial discharge impact tide in a convergent (turbid) tidal river. *Journal of Geophysical Research: Oceans*, *123*(5), 3241–3258. <https://doi.org/10.1002/2017jc013466>
- Jones, S., & Jago, C. (1996). Determination of settling velocity in the Elbe Estuary using quisset tubes. *Journal of Sea Research*, *36*(1–2), 63–67. [https://doi.org/10.1016/s1385-1101\(96\)90772-8](https://doi.org/10.1016/s1385-1101(96)90772-8)
- Jouanneau, J.-M., & Latouche, C. (1981). *The Gironde Estuary* (Vol. 10). Schweizerbart Science Publishers.
- Kim, K., Yoon, H.-S., Lee, I.-C., & Hibino, T. (2016). An influence of salinity on resuspension of cohesive sediment. *Journal of Coastal Research*, *75*(75), 68–72. <https://doi.org/10.2112/si75-014.1>
- Le, H.-A., Gratiot, N., Santini, W., Ribolzi, O., Tran, D., Meriaux, X., et al. (2020). Suspended sediment properties in the Lower Mekong River, from fluvial to estuarine environments. *Estuarine, Coastal and Shelf Science*, *233*, 106522. <https://doi.org/10.1016/j.ecss.2019.106522>
- Lee, B., Kim, J., Hur, J., Choi, I., Toorman, E., Fettweis, M., & Choi, J. (2019). Seasonal dynamics of organic matter composition and its effects on suspended sediment flocculation in river water. *Water Resources Research*, *55*(8), 6968–6985. <https://doi.org/10.1029/2018wr024486>
- Legout, C., Droppo, I., Coutaz, J., Bel, C., & Jodeau, M. (2018). Assessment of erosion and settling properties of fine sediments stored in cobble bed rivers: The Arc and Isère alpine rivers before and after reservoir flushing. *Earth Surface Processes and Landforms*, *43*(6), 1295–1309. <https://doi.org/10.1002/esp.4314>
- Liéart, C., Savoye, N., Bozec, Y., Breton, E., Conan, P., David, V., et al. (2017). Dynamics of particulate organic matter composition in coastal systems: A spatio-temporal study at multi-systems scale. *Progress in Oceanography*, *156*, 221–239. <https://doi.org/10.1016/j.pocan.2017.03.001>
- Lorrain, A., Savoye, N., Chauvaud, L., Paulet, Y.-M., & Naullet, N. (2003). Decarbonation and preservation method for the analysis of organic C and N contents and stable isotope ratios of low-carbonated suspended particulate material. *Analytica Chimica Acta*, *491*(2), 125–133. [https://doi.org/10.1016/s0003-2670\(03\)00815-8](https://doi.org/10.1016/s0003-2670(03)00815-8)
- Manning, A., & Dyer, K. (1999). A laboratory examination of floc characteristics with regard to turbulent shearing. *Marine Geology*, *160*(1–2), 147–170. [https://doi.org/10.1016/s0025-3227\(99\)00013-4](https://doi.org/10.1016/s0025-3227(99)00013-4)
- Manning, A., & Dyer, K. (2007). Mass settling flux of fine sediments in northern European estuaries: Measurements and predictions. *Marine Geology*, *245*(1–4), 107–122. <https://doi.org/10.1016/j.margeo.2007.07.005>
- Manning, A., Langston, W., & Jonas, P. (2010). A review of sediment dynamics in the Severn Estuary: Influence of flocculation. *Marine Pollution Bulletin*, *61*(1–3), 37–51. <https://doi.org/10.1016/j.marpolbul.2009.12.012>
- Manning, A., & Schoellhamer, D. H. (2013). Factors controlling floc settling velocity along a longitudinal estuarine transect. *Marine Geology*, *345*, 266–280. <https://doi.org/10.1016/j.margeo.2013.06.018>
- Markussen, T. N., & Andersen, T. J. (2014). Flocculation and floc break-up related to tidally induced turbulent shear in a low-turbidity, microtidal estuary. *Journal of Sea Research*, *89*, 1–11. <https://doi.org/10.1016/j.seares.2014.02.001>
- Mehta, A. J. (1986). Characterization of cohesive sediment properties and transport processes in estuaries. *Estuarine Cohesive Sediment Dynamics*, *14*, 290–325. https://doi.org/10.1007/978-1-4612-4936-8_15
- Mehta, A. J. (1989). On estuarine cohesive sediment suspension behavior. *Journal of Geophysical Research*, *94*(C10), 14303–14314. <https://doi.org/10.1029/jc094ic10p14303>
- Migniot, C. (1968). Etude des propriétés physiques de différents sédiments très fins et de leur comportement sous des actions hydrodynamiques. *La houille blanche*, *54*(7), 591–620. <https://doi.org/10.1051/lhb/1968041>
- Mikes, D., Verney, R., Lafite, R., & Belorgey, M. (2004). Controlling factors in estuarine flocculation processes: Experimental results with material from the Seine Estuary, northwestern France. *Journal of Coastal Research*, 82–89.
- Milligan, T. G., & Hill, P. (1998). A laboratory assessment of the relative importance of turbulence, particle composition, and concentration in limiting maximal floc size and settling behaviour. *Journal of Sea Research*, *39*(3–4), 227–241. [https://doi.org/10.1016/s1385-1101\(97\)00062-2](https://doi.org/10.1016/s1385-1101(97)00062-2)
- Nghiêm, J. A., Fischer, W. W., Li, G. K., & Lamb, M. P. (2022). A mechanistic model for mud flocculation in freshwater rivers. *Journal of Geophysical Research: Earth Surface*, *127*(5), e2021JF006392. <https://doi.org/10.1029/2021jfo06392>
- Osborn, R., Dillon, B., Tran, D., Abolfazli, E., Dunne, K. B., Nittrouer, J. A., & Strom, K. (2021). Floccarazi: An in-situ, image-based profiling instrument for sizing solid and flocculated suspended sediment. *Journal of Geophysical Research: Earth Surface*, *126*(11), e2021JF006210. <https://doi.org/10.1029/2021jfo06210>
- Osborn, R., Dunne, K. B., Ashley, T., Nittrouer, J. A., & Strom, K. (2023). The flocculation state of mud in the lowermost freshwater reaches of the Mississippi River: Spatial distribution of sizes, seasonal changes, and their impact on vertical concentration profiles. *Journal of Geophysical Research: Earth Surface*, *128*(7), e2022JF006975. <https://doi.org/10.1029/2022jfo06975>
- Pejrup, M. (1988). Flocculated suspended sediment in a micro-tidal environment. *Sedimentary Geology*, *57*(3–4), 249–256. [https://doi.org/10.1016/0037-0738\(88\)90032-2](https://doi.org/10.1016/0037-0738(88)90032-2)
- Pejrup, M., & Mikkelsen, O. A. (2010). Factors controlling the field settling velocity of cohesive sediment in estuaries. *Estuarine, Coastal and Shelf Science*, *87*(2), 177–185. <https://doi.org/10.1016/j.ecss.2009.09.028>
- Portela, L. I., Ramos, S., & Teixeira, A. T. (2013). Effect of salinity on the settling velocity of fine sediments of a harbour basin. *Journal of Coastal Research*, *65*, 1188–1193. <https://doi.org/10.2112/si65-201.1>
- Priya, K., Jegathambal, P., & James, E. (2015). On the factors affecting the settling velocity of fine suspended sediments in a shallow estuary. *Journal of Oceanography*, *71*(2), 163–175. <https://doi.org/10.1007/s10872-014-0269-x>
- Richardson, J., & Zaki, W. (1954). Sedimentation and fluidisation: Part 1. *Transactions of the Institution of Chemical Engineers*, *32*, 635–662.
- Ross, L., & Sottolichio, A. (2016). Subtidal variability of sea level in a macrotidal and convergent estuary. *Continental Shelf Research*, *131*, 28–41. <https://doi.org/10.1016/j.csr.2016.11.005>
- Ross, M., & Mehta, A. (1989). On the mechanics of lutoclines and fluid mud. *Journal of Coastal Research*, 51–62.
- Ross, M. A. (1988). *Vertical structure of estuarine fine sediment suspension (Unpublished doctoral dissertation)*. Coastal and Oceanographic Engineering Department, University of Florida.
- Savoye, N., David, V., Morisseau, F., Etcheber, H., Abril, G., Billy, I., et al. (2012). Origin and composition of particulate organic matter in a macrotidal turbid estuary: The Gironde Estuary, France. *Estuarine, Coastal and Shelf Science*, *108*, 16–28. <https://doi.org/10.1016/j.ecss.2011.12.005>
- Shi, Z., Zhou, H. J., Eitrem, S. L., & Winterwerp, J. C. (2003). Settling velocities of fine suspended particles in the Changjiang Estuary, China. *Journal of Asian Earth Sciences*, *22*(3), 245–251. [https://doi.org/10.1016/s1367-9120\(03\)00067-1](https://doi.org/10.1016/s1367-9120(03)00067-1)
- Sottolichio, A., & Castaing, P. (1999). A synthesis on seasonal dynamics of highly-concentrated structures in the Gironde Estuary. *Comptes Rendus de l'Académie des Sciences—Series IIA: Earth and Planetary Science*, *329*(11), 795–800. [https://doi.org/10.1016/s1251-8050\(00\)88634-6](https://doi.org/10.1016/s1251-8050(00)88634-6)

- Sottolichio, A., Hurther, D., Gratiot, N., & Bretel, P. (2011). Acoustic turbulence measurements of near-bed suspended sediment dynamics in highly turbid waters of a macrotidal estuary. *Continental Shelf Research*, 31(10), S36–S49. <https://doi.org/10.1016/j.csr.2011.03.016>
- Tang, F. H., & Maggi, F. (2016). A mesocosm experiment of suspended particulate matter dynamics in nutrient-and biomass-affected waters. *Water Research*, 89, 76–86. <https://doi.org/10.1016/j.watres.2015.11.033>
- Thill, A., Moustier, S., Garnier, J.-M., Estournel, C., Naudin, J.-J., & Bottero, J.-Y. (2001). Evolution of particle size and concentration in the Rhône river mixing zone: Influence of salt flocculation. *Continental Shelf Research*, 21(18–19), 2127–2140. [https://doi.org/10.1016/s0278-4343\(01\)00047-4](https://doi.org/10.1016/s0278-4343(01)00047-4)
- Van der Lee, W. (1998). The impact of fluid shear and the suspended sediment concentration on the mud floc size variation in the Dollard Estuary, The Netherlands. *Geological Society, London, Special Publications*, 139(1), 187–198. <https://doi.org/10.1144/gsl.sp.1998.139.01.15>
- van Leussen, W. (1994). *Estuarine macroflocs and their role in fine-grained sediment transport (Unpublished doctoral dissertation)*. University of Utrecht.
- van Leussen, W. (1999). The variability of settling velocities of suspended fine-grained sediment in the Ems estuary. *Journal of Sea Research*, 41(1–2), 109–118. [https://doi.org/10.1016/s1385-1101\(98\)00046-x](https://doi.org/10.1016/s1385-1101(98)00046-x)
- Van Maanen, B., & Sottolichio, A. (2018). Hydro-and sediment dynamics in the Gironde Estuary (France): Sensitivity to seasonal variations in river inflow and sea level rise. *Continental Shelf Research*, 165, 37–50. <https://doi.org/10.1016/j.csr.2018.06.001>
- Verney, R., Lafite, R., & Brun-Cottan, J.-C. (2009). Flocculation potential of estuarine particles: The importance of environmental factors and of the spatial and seasonal variability of suspended particulate matter. *Estuaries and Coasts*, 32(4), 678–693. <https://doi.org/10.1007/s12237-009-9160-1>
- Walch, H., Von der Kammer, F., & Hofmann, T. (2022). Freshwater suspended particulate matter—Key components and processes in floc formation and dynamics. *Water Research*, 220, 118655. <https://doi.org/10.1016/j.watres.2022.118655>
- Wendling, V. (2015). *Développement d'un système de caractérisation des agrégats et des floccs en suspension (Unpublished doctoral dissertation)*. Université Grenoble Alpes.
- Wendling, V., Gratiot, N., Legout, C., Droppo, I. G., Coulaud, C., & Mercier, B. (2015). Using an optical settling column to assess suspension characteristics within the free, flocculation, and hindered settling regimes. *Journal of Soils and Sediments*, 15(9), 1991–2003. <https://doi.org/10.1007/s11368-015-1135-1>
- Winterwerp, J. C. (1998). A simple model for turbulence induced flocculation of cohesive sediment. *Journal of Hydraulic Research*, 36(3), 309–326. <https://doi.org/10.1080/00221689809498621>